

Contact study between fiber and matrix in composite materials

Júlio A. S. Neto¹, Luiz C. Wrobel¹

¹*Civil and Environmental Engineering Department, Pontifical Catholic University of Rio de Janeiro
Rua Marquês de São Vicente, 225 – Gávea – Rio de Janeiro – Brazil
julioneto7@aluno.puc-rio.br, luiz.wrobel@puc-rio.br*

Abstract. Composite materials are widely used in engineering, and can be exemplified with reinforced concrete, one of the main inputs of civil construction. Given its importance in the area, the contact behavior between the components of these materials was studied, that is, between the matrix and the inclusions. Thus, this paper presents a study of how different parameters influence the distribution of internal stresses in composites due to external loads. Several computational models were analyzed using the finite element method, in models with only one inclusion (fiber or particle), which were evaluated considering how different values of the modulus of elasticity, Poisson's ratio and friction coefficient influence the stress concentrations present in the contact between inclusion and matrix. Furthermore, the models were analyzed under two premises, one where there is a possible detachment between the matrix and the inclusions and another where the contact is fully-Bonded. The graphics elaborated from the results of these models clearly show the influence of the various parameters studied, whose the performed analysis can be used for the production of increasingly efficient composite materials

Keywords: Finite Element Method, Contact mechanics, Composite materials.

1 Introduction

There are many situations in engineering in which a single material does not meet the needs of the studied problem. To overcome this problem, it is common to make a combination between different materials that together present a different behavior than when they are separated. Thus, the composite material made from this combination improve the properties of their base materials.

Even with composite materials being used for a long time, Gibson [1] stated that it was around the 1960s that studies began to be made to determine the behavior of this type of material. Hence, there are still many aspects to be studied about composite materials, such as the interaction between their constituents.

This interaction is studied mainly by the mechanics of contact. Barber and Ciavarella [2] stated that this area of study is fundamental to study solids because it is through contact that loads are transferred and, besides, the contact is one of the main causes of stress concentration inside the composites. Despite being something fundamental and present in practically all types of situations, Wriggers [3] stated that the study on contact is complex and requires research to define its behavior.

2 Models description

The problem studied in this article is related to the determination of the contact between spherical inclusions (particles) or cylindrical inclusions (fibers) and the matrix. Circular inclusions were studied because they are the most common and most used in practice. These stresses were determined according to the following parameters:

- Ratio between the modulus of elasticity (E_i/E_m), where the index i refers to the inclusion and the index m refers to the matrix;
- Ratio between the Poisson's ratio (ν_i/ν_m);
- Friction coefficient (μ) between the contact faces.

The models were made with the aid of the ABAQUS software. The spherical inclusions were simulated with an axisymmetric model, while the fibers were represented by a plane stress model. In both cases, the composite cross section was modeled.

For models which the fully-Bonded contact was adopted, that is, when the matrix and the fiber do not come off, a tie constraint was used, which was configured to ensure that there was no relative displacement between the contact faces of the fiber and the matrix. For this boundary condition it was assumed that the face of the matrix was the master and the face of the fiber, the slave.

Regarding the models which the separation between the inclusion and matrix faces is allowed, a hard contact condition was used that prevented the faces from crossing. This relationship minimizes penetration of the slave surface on the main surface at the restriction sites. The same master and slave considerations were made as in the previous model.

Since the model is symmetrical on both the x and y axis, it was possible to model only a quarter of the structure using symmetry boundary conditions, as illustrated by Figure 1. In addition, since the objective of this work is to study the stresses in the contact between the fiber and the matrix, the finite element mesh is more refined in this region of greatest interest, as illustrated in Figure 1. In this model, the matrix side is four times larger than the inclusion radius, the mesh has about ten thousand 6-node modified quadratic axisymmetric triangle elements. The loads used are static. θ and φ are the angles along the contact face.

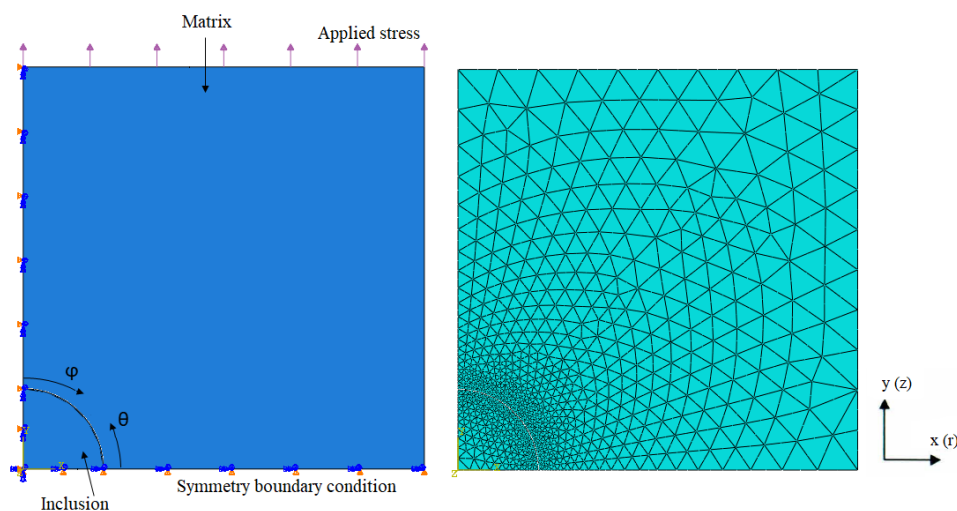


Figure 1. Typical 2D Finite Element model of a single fiber/particle within a finite matrix under an externally applied load.

3 Fully-Bonded Problem

To assess the influence that each parameter has on the internal stresses of the composite, it was decided to use normal stresses on the contact face. For this purpose, it was created a cylindrical axis originated from the center of the inclusion, and thus the main stress (S22) represented the normal stresses along the contact face between the fiber and the matrix. Figure 2 illustrates this stress map.

It is possible to notice that the normal stresses on the contact face were higher in the composite with particles. Also, the normal stresses are higher near the vertical axis, which are tensile stresses, and decrease along the face until they present compression stresses near the X axis.

3.1 Effect of Relative Inclusion Stiffness

The first parameter evaluated was the ratio between the modulus of elasticity of inclusion and matrix. Four E_i/E_m ratios were evaluated, 0.1, 1.0, 10 and 100. In these models, no variations were made in the Poisson's ratio or geometry. From the results of the numerical models, the graph illustrated in Figure 3 was made, which shows the normal stresses along the contact face between inclusion and matrix, for fiber and particle. The stresses were normalized according to the tensile forces applied to the structure.

As already mentioned, the models were solved using the finite element method (FEM) and these results are presented in the graph by continuous lines. To validate the models, these results were compared with those obtained by Knight [4] using the boundary element method (BEM), presented in the graph by the dotted lines.

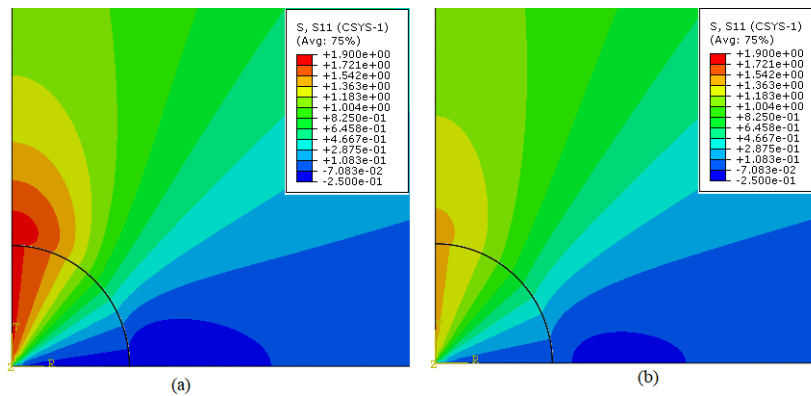


Figure 2. Contour plot indicating normal stresses on the contact face for (a) particle and (b) fiber. (Fully-bonded, $E_i/E_m = 10$ and $\nu_i = \nu_m = 0.3$)

It is seen that the results obtained were good, showing a difference of less than 10% between the compared values. This error can be justified by the considerations used in the contact between the faces of the matrix and inclusion, or by the difference in the methodologies used to solve the models, in addition to the fact that the BEM values were captured manually from the chart published by Knight [4].

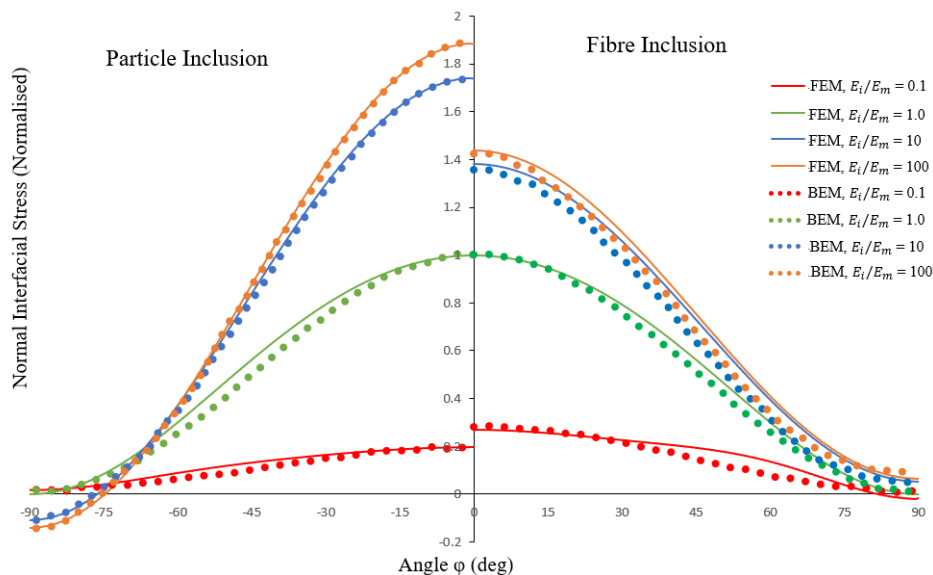


Figure 3. Effect of the elastic moduli ratio (E_i/E_m) on the normal interfacial stress distribution under uniaxial tension. (Fully-bonded, $\nu_i = \nu_m = 0.3$)

According to the presented graph, it was noticed that the stresses behave in similar ways for both the fiber and the particle. The greatest stresses are located at angle $\varphi = 0^\circ$, which are tensile stresses. In addition, as the inclusion becomes more rigid ($E_i > E_m$), the stresses increase and small compression stresses close to $\varphi = 90^\circ$ arise due to the contraction of the matrix perpendicular to the applied load caused by the Poisson’s ratio.

3.2 Effect of Poisson’s Ratio

In the previous models, the Poisson’s ratio of the inclusion and the matrix were the same. Therefore, it was studied how the normal stress at the contact face between the matrix and the inclusion varies when the inclusion has a higher Poisson ($\nu_i/\nu_m = 2$) and the inverse situation ($\nu_i/\nu_m = 0.5$).

Figure 4 presents the data obtained from these models. For both the fiber and the inclusion, it was noticed that the stresses are greater when the Poisson’s ratio is greater in the inclusion, while the stresses are lower when

the Poisson’s ratio of the matrix is greater. It is also notable that the particle was more sensitive to this change, as it showed variations of up to 19% while the fiber showed a variation of 4% for the same point.

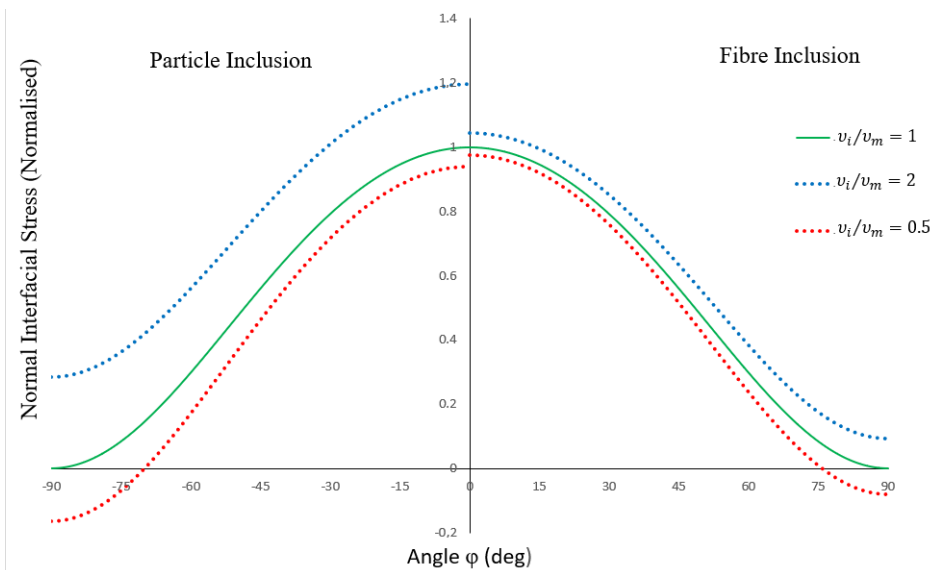


Figure 4. Effect of a Poisson’s ratio mismatch (v_i/v_m) on the normal interfacial stress distribution (an) under uniaxial tension. (Fully-bonded, $E_i/E_m = 1$)

4 Non-Bonded (Contact) Problem

The non-Bonded contact models are those that allow the detachment between the contact faces of the inclusion and matrix. Figure 5 illustrates the map of principal stresses in the y direction (S22), the same direction of application of the loads, for both the particle model and the fiber model. The ratio between the modulus of elasticity (E_i/E_m) is equal to 10 and the Poisson’s ratio is equal to 0.3 for both materials.

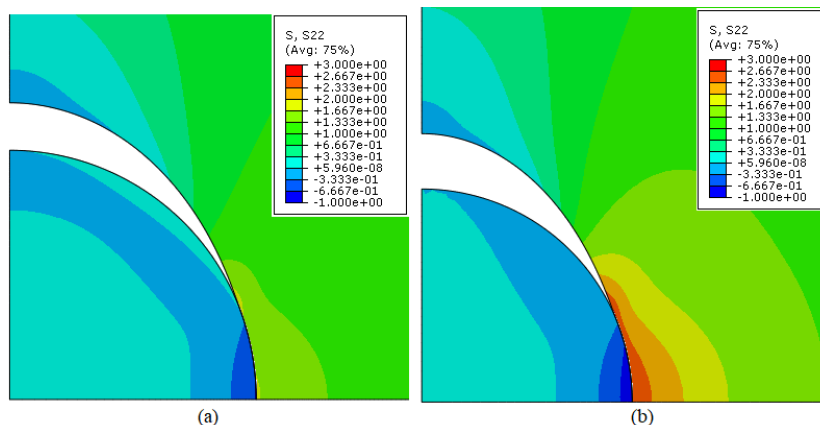


Figure 5. Contour plot indicating the variation of second principal stress (S22) within the particle (a), and fiber (b) inclusion model. (Non-bonded, $E_i/E_m = 10$, $v_i = v_m = 0.3$, $\mu = 0$)

For this model, where there is a detachment between the materials, it is noticed that the main stresses are higher in the fiber reinforced composite, differently from the previous situation, where the contact was fully-bonded. It is visible that the inclusions started to experience compressive stresses on the sides, especially where the contact was maintained with the matrix. This can be explained by the Poisson effect, since the matrix is stretching vertically and retracting horizontally. The points with greatest stress concentrations occur at the points where the separation between the materials begins, which occurs close to the angle $\theta = 20^\circ$.

4.1 Effect of Relative Inclusion Stiffness

To study the influence that the ratio between the modulus of elasticity (E_i/E_m) present in these composites, models with different ratios were made, namely 0.1, 1, 10 and 100. The geometry is the same in both models, as well as the Poisson's ratio of 0.3. Figure 6 presents the results obtained for normal stresses along the contact face for the different ratios already mentioned.

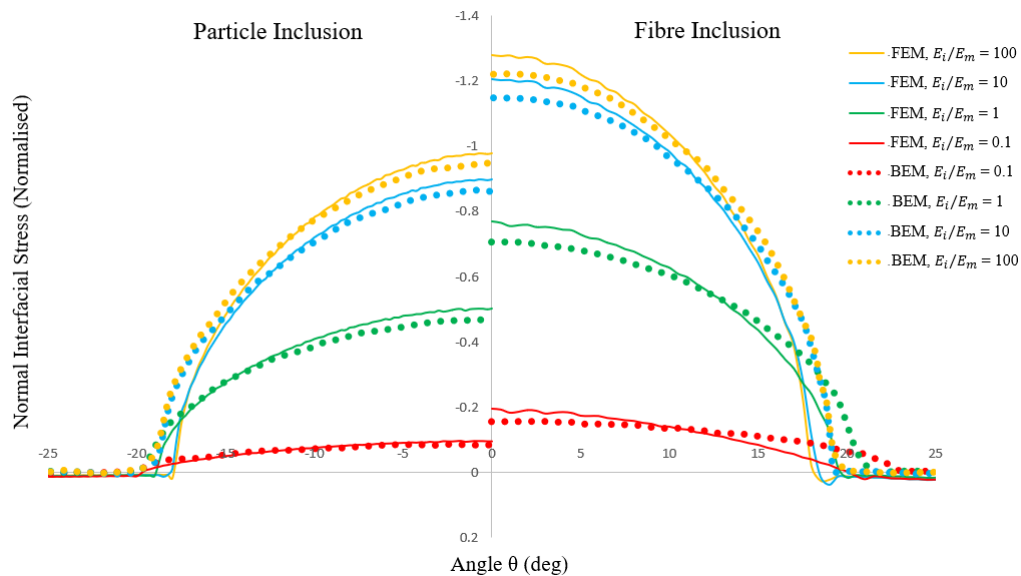


Figure 6. Effect of the elastic moduli ratio (E_i/E_m) on the normal contact stress distribution under uniaxial tension. (Non-bonded, $\nu_i = \nu_m = 0.3$, $\mu = 0$)

Again, the results obtained were compared with the data presented by Knight et al. [5] for validation of the study. Figure 6 illustrates that the developed models presented good results, showing a difference of less than 10% between the compared values.

From the results obtained for these models where there is detachment, it was observed the presence of compressive stresses. It is also seen that the greater the ratio between the inclusion elasticity modulus and the matrix (E_i/E_m), that is, the more rigid the inclusion, the higher the stresses are, in addition to the fact that the contact angle becomes smaller. It is visible that the stresses in the fibers are higher in all cases, compared to the stresses in the particle.

4.2 Effect of Poisson's Ratio

Then models were made to evaluate the effect that the Poisson's ratio can have on normal stresses in non-bonded contact. The first evaluation was made for three different values of the Poisson's ratio. The inclusion and the matrix had the same value for this coefficient, that is, there was no variation of the Poisson's ratio within the same composite. The values used were 0, 0.3 and 0.49 and Figure 7 illustrates the results obtained from the numerical models.

From the presented graph it is seen that composites reinforced with particles are very sensitive to changes in the Poisson's ratio of the materials, since for the three values evaluated, there was a difference of up to 51% between the stresses obtained, where the stresses are higher for coefficients of higher Poisson's ratio. In addition, the angle at which the components come off is smaller as the Poisson's ratio decreases. In turn, the models reinforced with fibers showed almost zero variation under the same conditions.

4.3 Effect of Frictional Contact Conditions

The first models were made for fully-bonded contact, that is, there was no relative displacement between the contact faces of the inclusion and the matrix; therefore, it was not possible to evaluate the effect of friction. In turn,

for non-bonded contact models, this study is possible. Thus, models with different friction coefficients were made to assess its effect on the normal stresses on the contact face. The friction coefficients used were 0 (frictionless condition used as a reference), 1 and 5, arbitrarily chosen. Figure 8 illustrates the data obtained from the numerical models.

It is observed that the behavior of normal stresses along the face has become more irregular in both cases, both for the particle and for the fiber and as the friction has increased, the stresses have decreased. It is also seen that for cases where the friction coefficient (μ) is equal to 1, the maximum stress was not located close to the angle $\theta = 20^\circ$. Also, the contact angle is slightly higher for larger friction coefficients.

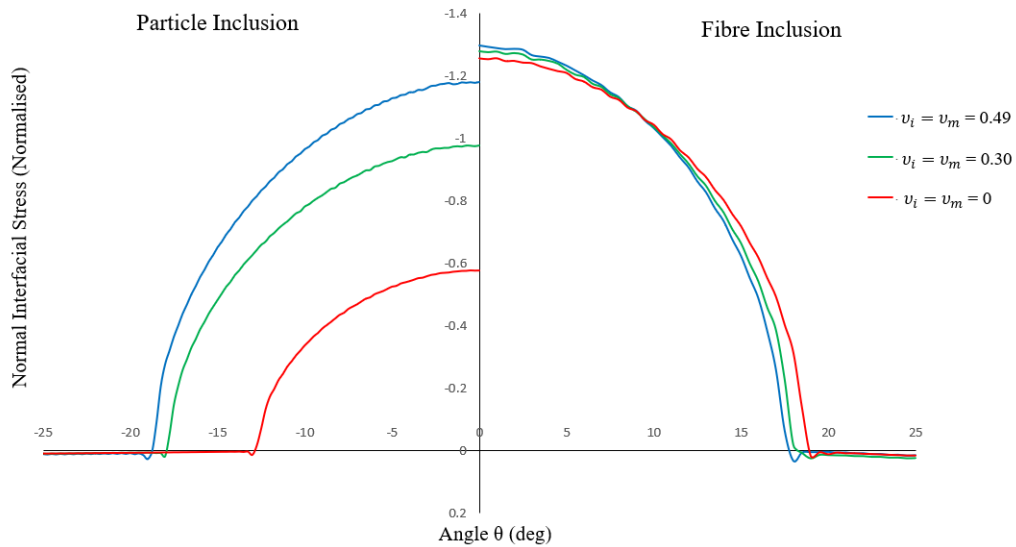


Figure 7. Effect of the Poisson's ratio (ν) on the normal contact stress distribution under uniaxial tension. (Non-bonded, $E_i/E_m = 100$, $\mu = 0$)

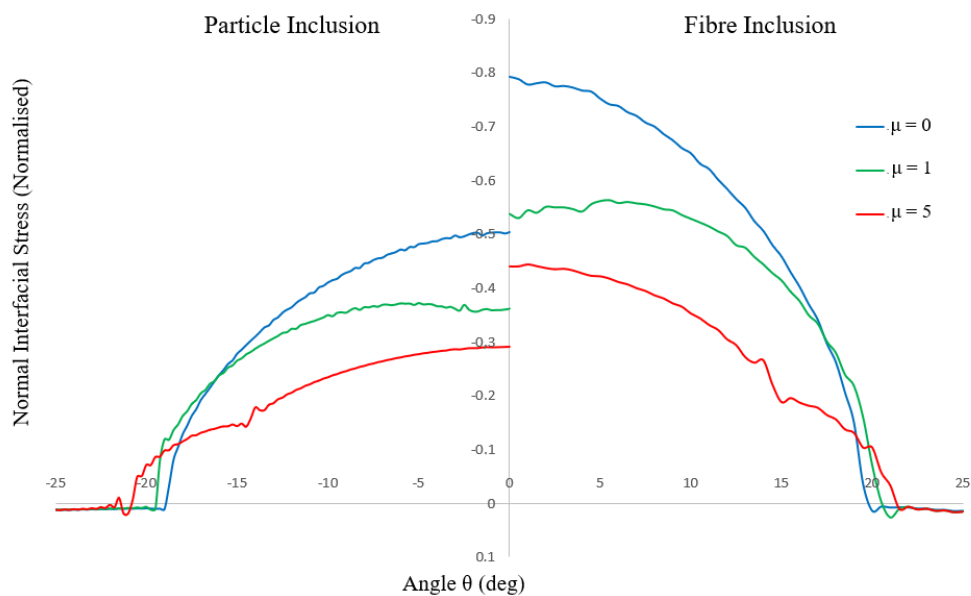


Figure 8. Effect of the friction coefficient (μ) on the normal stress distribution under uniaxial tension. (Non-bonded, $E_i/E_m = 1$, $\nu_i = \nu_m = 0.3$)

5 Conclusions

This paper studied how some parameters influence the contact stresses between inclusion and matrix in composite materials. These studies were done for problems with fully-bonded and non-bonded contact. The models with fully-bonded contact showed that as the ratio between the inclusion and matrix modulus of elasticity (E_i/E_m) increases, the stresses tend to be higher. In addition, for the corresponding models, the stresses in the particle are higher than the stresses around the fiber. Furthermore, the incompatibility between the Poisson's coefficients slightly affects the stresses along the contact face, so that when the inclusion is more rigid than the matrix ($\nu_i > \nu_m$) the stresses are slightly higher, while for more flexible inclusions ($\nu_i < \nu_m$) the stresses are slightly lower. This is valid for both inclusions, fibers and particles.

In turn, for the models with non-bonded contact, it was seen that the compression stresses on the contact face between the inclusion and the matrix increase as the ratio between the modulus of elasticity (E_i/E_m) increases, this is valid for both fiber and particle. For the corresponding models, fiber composites have higher compressive stresses than particles. In addition, the particle models were overly sensitive to changes in the Poisson's ratio. When there is compatibility between the particle and matrix coefficients, the stresses and the contact angle increase as the Poisson's ratio increases, reaching more than 50% within the studied range. For fiber composites, however, changes in the Poisson's ratio have no significant influence. Finally, the compressive stresses were shown to be lower with the consideration of friction, for both fiber and particle, in addition to the fact that the contact angle tends to increase with the increase of the friction coefficient.

Acknowledgements.

The authors acknowledge PUC - Rio for their support during the development of this study and CAPES (Coordenação de Aperfeiçoamento de Pessoal de Nível Superior) and CNPq (Conselho Nacional de Desenvolvimento Científico e Tecnológico) for their continued financial support.

Authorship statement.

The authors hereby confirm that they are the sole liable persons responsible for the authorship of this work, and that all material that has been herein included as part of the present paper is either the property (and authorship) of the authors, or has the permission of the owners to be included here.

References

- [1] GIBSON, R. F., 2016. *Principles of composite materials mechanics*. Florida.
- [2] BARBER, J. R.; CIAVARELLA, M., 2000. Contact mechanics. *International Journal of Solids and Structures*, vol. 37, pp. 29–43.
- [3] WRIGGERS, P., 2006. *Computational Contact Mechanics*. The Netherlands.
- [4] KNIGHT, M. G., 2002. *Numerical modelling of particulate and fibre reinforced composites*. PhD Thesis, Brunel University London, Brunel, UK.
- [5] KNIGHT, M. G.; LACERDA, L. A.; HENSHALL, J. L.; WROBEL, L. C., 2002. Parametric study of the contact stresses around spherical and cylindrical inclusions. *Computational Materials Science*, vol. 25, pp. 115–121.